Int. J. Electrochem. Sci., 8 **(2013)** 6524 - 6534

International Journal of
ELECTROCHEMICAL
SCIENCE
www.electrochemsci.org

Layer-by-Layer Assembled Multilayer Films of Nitrogen-doped Graphene and Polyethylenimine for Selective Sensing of Dopamine

Nana Li[1], *Enhui Zheng*[1], *Xia Chen*[1], *Shuorong Sun*[1], *Chunping You*[2], *Yongming Ruan*[1*] *and Xuexiang Weng*[1*]

[1]College of Chemistry and Life Science, Zhejiang Normal University, Jinhua 321004, China.
[2]State Key Laboratory of Dairy Biotechnology, Technology Center, Bright Dairy and Food Co. Ltd., Shanghai 200436, China
[*]E-mail: ruanym@zjnu.cn; xuexian@zjnu.cn

Received: 3 March 2013 / *Accepted:* 23 March 2013 / *Published:* 1 May 2013

A novel sensor was developed based on the electrostatic layer-by-layer (LBL) self-assembly technique on a glassy carbon electrode (GCE) modified with nitrogen-doped graphene (NG) and polyethylenimine (PEI). Electrochemical studies exhibit that the assembled NG multilayer films have favorable electron transfer ability and electrocatalytic property, which could enhance the response signal towards dopamine (DA) in the presence of ascorbic acid (AA). In addition, the self-assembly electrode possess an excellent sensing performance for the detection of dopamine with a linear range from 1.0×10^{-6} M to 1.3×10^{-4} M, and the detection limit is 5×10^{-7} M (S/N=3).

Keywords: Nitrogen-doped graphene, Layer-by-Layer, Sensor, Dopamine.

1. INTRODUCTION

Dopamine (DA) [1], a simple organic chemical in the catecholamine family, is a monoamine neurotransmitter. Abnormal levels of DA are related to neurological disorders, such as schizophrenia and Parkinson's disease [2, 3]. Because of the important physiological roles in the mammalian central nervous system, extensive research [4] has been conducted into the development of reliable DA determination methods. Electrochemical detection based on its oxidation has proven to be simple, fast, and sensitive. The major problem of DA electrochemical determination is the interference from ascorbic acid (AA), which usually coexists with DA in real systems in large amount [5, 6]. Therefore, electroactive materials having catalytic effect on the oxidation of DA have been sought to restrain from

the voltammetric response overlap of AA. Nanomaterials, such as gold nanoparticles [7-9], fullerenes [10], carbon nanotubes [11-13] and graphene [14-17] have shown the fantastic applications in bioelectronics and biosensing owning to their chemical inertness, relatively wide potential window, low background current and suitability for different types of analysis. Several reviews [18, 19] have focused on the biosensing applications of the nanomaterials.

Recently, researches have shown that nitrogen-doping of graphene (NG) is an effective and intrinsically modified method to enhance the graphene performance in superconductors, nanogenerator, field-effect transistor and lithium ion batteries systems [20, 21]. The neighbor nitrogen dopants tailor the electronic properties, manipulate the surface chemistry, and induce the "activation region" of the graphene surface [22]. Therefore, NG provides strong potentials in electrochemical sensing and other electrocatalytic applications. Most recently, there have been several investigations concerning the electrocatalytic performance of NG. Xia and coworkers [23] utilized NG-based electrode to simultaneously determine AA, DA and uric acid. Wang et al. [24] observed that NG sheets exhibited excellent selectivity and sensitivity for glucose with concentrations as low as 0.01 mM in the presence of interferences. Xiong et al. [25] found that the Pt/NG catalysts exhibited significantly higher electrochemical catalytic activity for the oxidation of methanol compared to their analogous undoped NG. Among these work, sensing films of NG were constructed with directly casting on the sensing base. In brief, these findings reveal that the uniqueness of NG as a sensing film is beginning to emerge and the film formation technique needs to be fully developed for more extensive applications.

The layer-by-layer (LBL) assembly technique has been widely developed as one of the most powerful techniques to prepare multifunctional films with desired functions, structures and morphologies because of its versatility in the process steps in both material and substrate choices [26]. Herein, we prepare stably assembled NG multilayer films using LBL method based on electrostatic interaction between the positively charged polyethylenimine (PEI) and negatively charged NG to study electrochemical catalytic activity of DA. The remarkable sensitivity and selectivity of the assembled electrode was realized in the presence of excess of AA compared with the case of a bare GC electrode.

2. EXPERIMENTAL

2.1. Reagents and instruments

Graphite powder (99.9995% purity), was purchased from Alfa Aesar. Ascorbic acid was bought from Sinopharm Chemical Reagent CO. Ltd (China). Dopamine was bought from Sigma and used as received. Polyethylenimine (PEI, M.W. 70,000) was purchased from the Chemical Reagent Company of Shanghai (Shanghai, China). Phosphate buffer solution (PBS) was prepared using stock solutions of 0.1 M Na_2HPO_4 and 0.1 M NaH_2PO_4. All other chemicals were of analytical grade, and double distilled water was used throughout the experiments.

All electrochemical measurements were performed on a CHI 660C electrochemical workstation (Chenhua Instrument Co. Shanghai, China). A conventional three-electrode electrochemical cell was

used, a modified glass carbon electrode (GCE, diameter 3.0 mm) as the working electrode, a saturated calomel electrode (SCE) as the reference electrode and a platinum wire as the auxiliary electrode.

The surface morphology of the LBL films was characterized using scanning electron microscopy (SEM, Hitachi S-4800, Japan). A silicon wafer was used for SEM characterization to mimic a GCE surface. The surface was first cleaned in a piranha solution (a 1:3 mixture of 30% H_2O_2 and concentrated H_2SO_4) and then thoroughly rinsed with distilled water. The pretreated silicon wafer was alternatively immersed in the solutions of NG and PEI, rinsed with water, and then dried in a stream of nitrogen.

2.2. Synthesis of nitrogen doped graphene

Typically, 20 mL of 1 mg/mL graphene oxide [27] solution was adjusted the pH value to 10 using 30% ammonia under magnetically stirring for 10 min. The solution was then transferred into a Teflon-lined autoclave and heated at 120 °C for 12 h. The as-prepared nitrogen-doped graphene sheets kept static to cool down, then collected with centrifugation, followed by washing with deionized water and ethanol for three times, and then dried at 60ºC for 6 h. For comparison, graphene was also synthesized [28] in the same hydrothermal conditions with 0.1 M NaOH (pH =10).

2.3. Preparation of assembled films

GCE was used to grow the multilayer films. Prior to modification, GCE was polished to get a mirror surface with 0.3 and 0.05 μm alumina powder sequentially and then washed with ultrasonication in water and ethanol for 3 min, respectively. NG was dispersed in DMF by ultrasonication, and resulted in 1 mg/mL suspension. The procedure for preparing the multilayer film was as follows. First, the polished electrode was dipped into the solution of NG for 30 min. After being rinsed in distilled water to remove the excess of assembling material and then dried with N_2 gas flow, the negatively charged NG modified electrode was immersed into the positively charged PEI (3 % w/v) for 30 min and rinsed. The cycle was repeated five times to obtain $(NG/PEI)_5$ mutilayer films. The films-modified electrode is henceforth designated as $(NG/PEI)_5$/GCE.

3. RESULTS AND DISCUSSION

3.1. Film characterization

Raman spectra (Fig. 1) are employed to show the electronic and phonon structure of the as-synthesized graphene and NG. Both materials display two peaks at about 1360 and 1600 cm^{-1}, which are corresponded to the D band (the defect-related peak due to the reduction in size of the in-plane sp^2 domains) and G band (assigned to the E_{2g} phonon mode of sp^2 hybridized carbon atoms), respectively [29,30]. In contrast, the G band of NG shifted downward to 1592 cm^{-1} with an increased strength ratio

of D band to G band (I_D/I_G), inferring the increase of the number of defects caused by nitrogen doping [20].

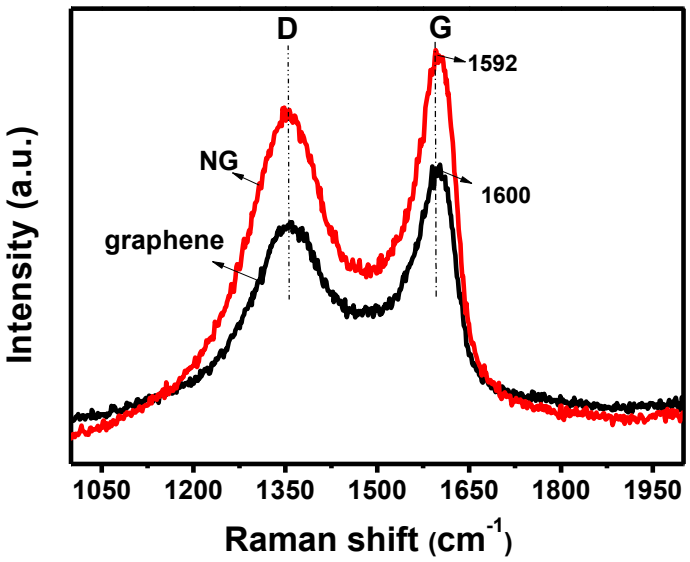

Figure 1. Raman spectra of graphene and NG.

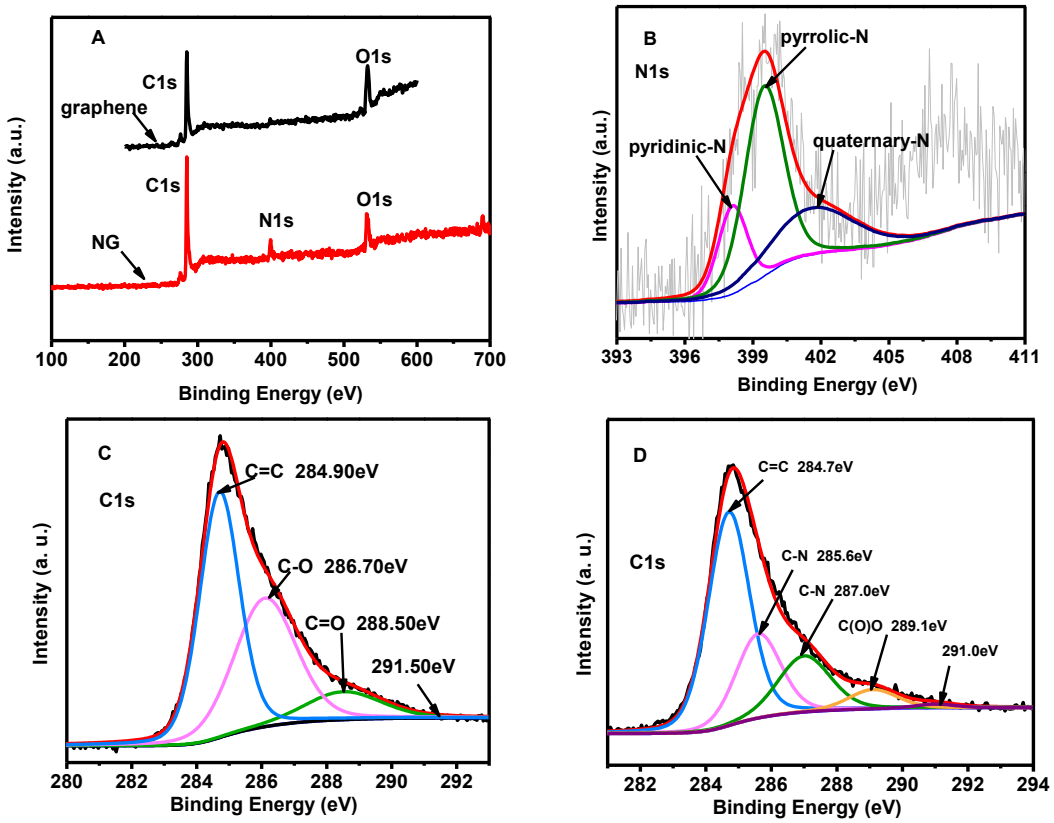

Figure 2. (A) XPS survey scan of graphene and NG, (B) high-resolution N1s spectra of NG, C1s spectra of (C) graphene, and (D) NG.

The nitrogen bonding configurations of graphene and NG were further carried out using X-ray photoelectron spectroscopy (XPS). From the XPS general survey scan of NG (Fig. 2A), not only the presence of the C and O elements is revealed by the spectrum, also the existence of N1s can be recognized. Meanwhile, the amount of nitrogen in NG is determined to be 8.27%. In the deconvoluted N1s spectrum (Fig. 2B), the binding energy values of 398.1 eV, 399.5 eV and 401.6 eV are assigned to pyridinic N, pyrrolic N, and quaternary N (also called "graphitic nitrogen"), respectively [31]. Moreover, the deconvoluted C1s spectrum of NG (Fig.2D) is not just the same as that of the graphene (Fig. 2C) which shows one main peak at 284.7 eV (C=C) and four small peaks at higher binding energy, indicating the existence of C–N, C–OH and C=O bonds [32]. Above results reveal that nitrogen atoms have been successfully incorporated into graphene frameworks.

The hydroxyl and amine groups produced on NG surface make NG negatively charged in aqueous solution [33] and it can electrostatically interact with the positively charged polyelectrolyte PEI. Fig. 3A displays the SEM image of the layer-by-layer alternative growth of such NG and PEI films. It can be seen that the substrate is densely covered with homogenous NG with lots of ripples after five layers of NG and PEI were assembled. For comparison, SEM images of NG alone and PEI alone are also given. As seen in Fig. 3B, with the lack of electrostatic interaction, the distribution of the products is less uniform and most of the surface is free of coverage.

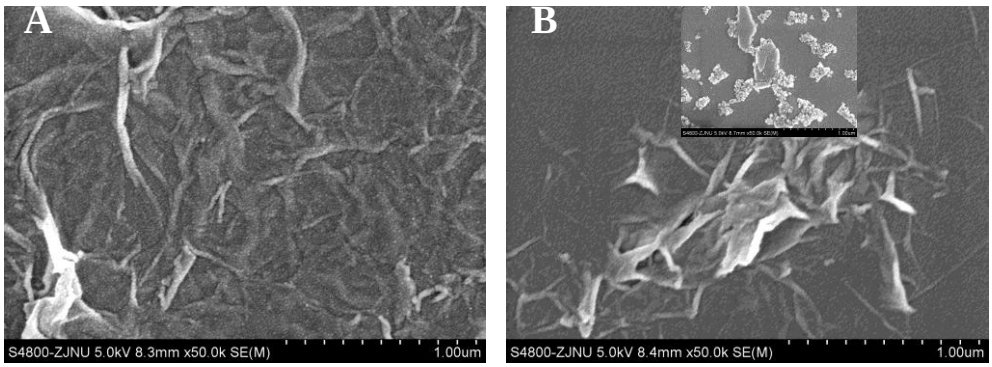

Figure 3. SEM images of (A) $(NG/PEI)_5$, (B) NG alone, and PEI alone (B, inset) confined on a silicon wafer.

3.2.Electrochemical properties of $(NG/PEI)_5$ modified GCE

Equivalent 5.0 mmol L^{-1} $[Fe(CN)6]^{3-/4-}$ redox couple was used to investigate the interface properties of the modified electrodes. Fig. 4A shows the cyclic voltammograms (CVs) response of $[Fe(CN)6]^{3-/4-}$ at bare GCE and $(NG/PEI)_5$/GCE. The bare GC electrode gives the reversible electrochemical response for the probe. Compared with the bare electrode, CV of $(NG/PEI)_5$/GCE shows better reversible response with a smaller peak-to-peak potential difference and an increased peak current intensity. The results indicate that the LBL modified electrode possesses the essential surface structure and electronic properties to support the rapid electron transfer in this redox system. Such an enhancement in the electron transfer kinetics was also found in electrochemical impedance measurements. As shown in Fig. 4B curve a, a small semicircle at high frequencies and an almost

straight line at low frequencies, which is a characteristic of a diffusion limited step of the electrochemical process, are observed at the bare GCE. The semicircle diameter of electrochemical impedance spectroscopy is equal to the electron transfer resistance, depending on the insulating and dielectric features at the electrode and electrolyte interface. As expected, after the modification of $(NG/PEI)_5$ multilayers, $(NG/PEI)_5$/GCE shows an almost straight tail line. The results above indicate that the presence of NG nanomaterial could facilitate the electron transfer [23].

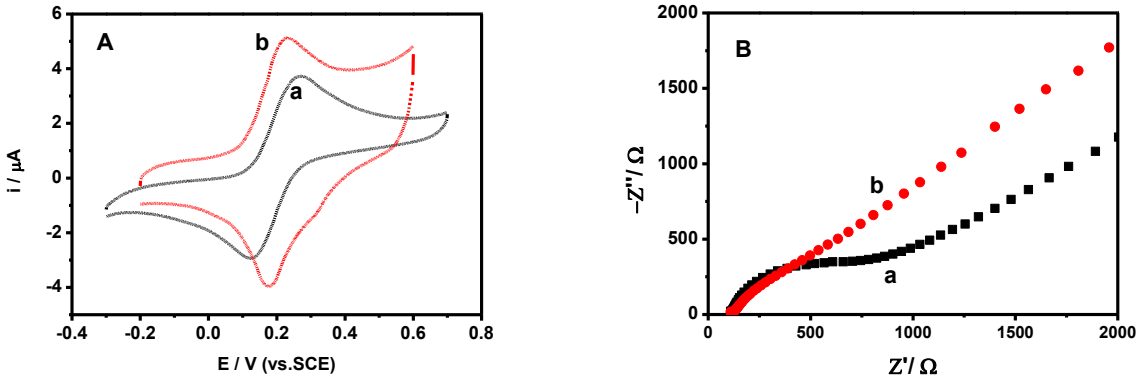

Figure 4. (A) CVs and (B) electrochemical impedance spectroscopy of GCE (curve a) and $(NG/PEI)_5$/GCE (curve b) in 2.5 mM $[Fe(CN)_6]^{3-}$/ $[Fe(CN)_6]^{4-}$ containing 0.1 M KCl. The frequency range was from 0.01 to 10^5 Hz with perturbation amplitude of 5 mV. The initial potential is 0.16 V.

3.3 Electrochemical oxidation of DA and AA at modified electrodes

Fig. 5A depicts the oxidation of DA at the $(NG/PEI)_5$/GCE and bare GCE in 0.1M PBS (PH=7.4). The redox behavior of DA has been established to undergo a two-electron and two-proton process [34] (scheme 1, Eq. (1)). The cathodic and anodic peaks were located at 0.063 and 0.216 V, respectively, showing a smaller peak-to-peak separation (ΔE= 153 mV) than that at bare GCE (ΔE= 215 mV). The anodic peak currents obtained at the assembled electrode is 28 μA, which is larger than that of bare GCE. A remarkable catalytic activity of the assembled electrode was also found for the redox process of AA (Fig. 5B). The redox behavior of AA has documented to be a one-proton and two-electron process [34] (scheme 1, Eq. (2)), which occurs with a small overpotential at $(NG/PEI)_5$/GCE, indicating the fast electron transfer rate.

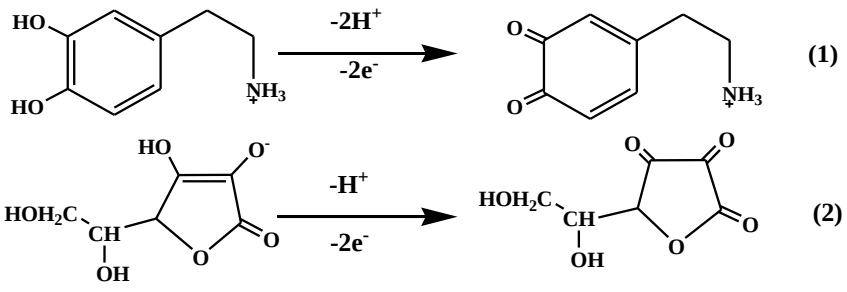

Scheme 1. The proposed electrochemical oxidation process of DA (1) and AA (2) in neutral solution.

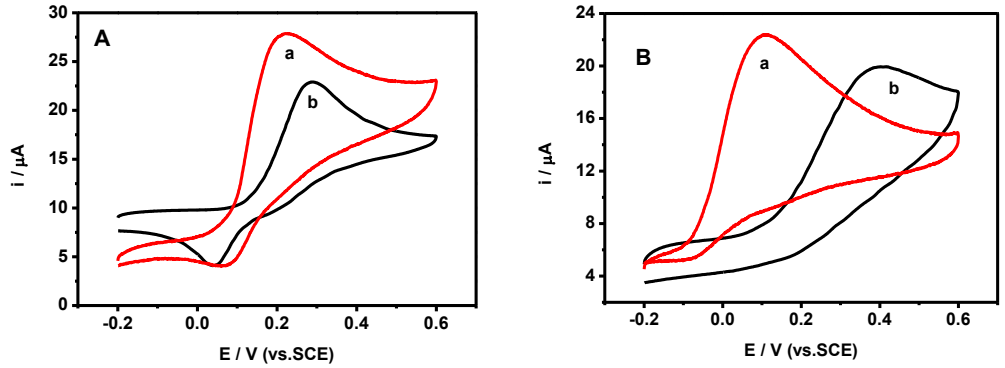

Figure 5. CVs of 1mM (A) DA and (B) AA at $(NG/PEI)_5$/GCE (curve a) and bare GCE (curve b) in 0.1M PBS (PH=7.4) with a scan rate of 100 mV/s.

Differential pulse voltammetry (DPV) was used for further investigate the electrocatalytic behavior of DA and AA at $(NG/PEI)_5$/GCE. Fig. 6 presents the DPV curves at different electrode for the oxidation of 60 μM DA in the presence of 5 mM AA in PBS (pH=7.4) solution. Only one weak and broad peak was observed at the bare GCE (curve b), while at $(NG/PEI)_5$/GCE (curve a) the merged voltammetric peak can be effectively resolved into two well-defined oxidation peaks with respect to AA and DA oxidation appeared at -0.050 V and 0.11 V, respectively. CV and DPV experiments demonstrate that compared to bare GCE, NG/PEI assembled electrode shows good electrocatalytic activity towards the oxidation of DA and AA. The sluggish electron transfer rate at bare GCE might be attributable to the electrode fouling, which caused by the deposition of oxidation product of AA at bare electrode, which could be anticipated to be well avoided at the NG assembled GCE because NG with oxygen- and nitrogen-containing groups at the open ends possesses strong ability against adsorption [23]. The control experiments with PEI alone (curve c) and NG alone (curve d) modified electrodes show that the simultaneous determination of DA and AA could not be efficiently realized. The results reveal that the uniform and compact films caused by electrostatic interaction result in excellent electrocatalysis towards DA and AA.

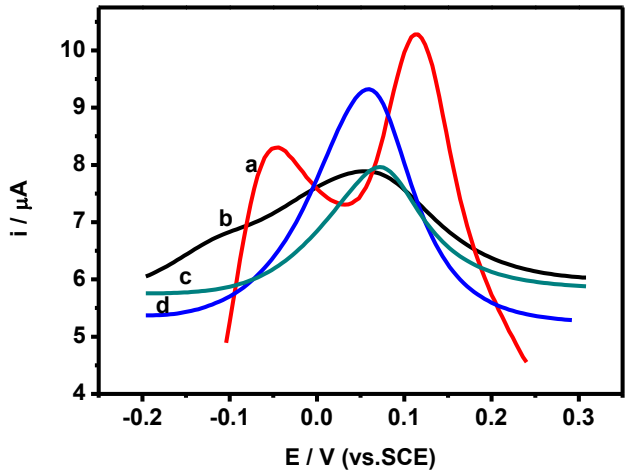

Figure 6. DPVs for 0.06 mM DA and 5 mM AA in 0.1M PBS (pH 7.4) at $(NG/PEI)_5$/GCE (a), bare GCE (b), PEI alone (c) and NG alone (d) modified electrode, respectively.

3.4. Effect of scan rate on the electrochemistry of AA and DA

The effect of scan rate on the CV responses of AA and DA at the $(NG/PEI)_5$/GCE was investigated and the results are shown in Fig. 7. The oxidation peak currents of DA and AA increase with increasing the scan rate, while their oxidation peak potentials gradually shift to positive values. Plots of the anodic peak currents as a function of the square root of scan rate in the range of 20-500 mV/s show linear relationships, which indicates the electrode reactions of DA and AA are diffusion - controlled processes.

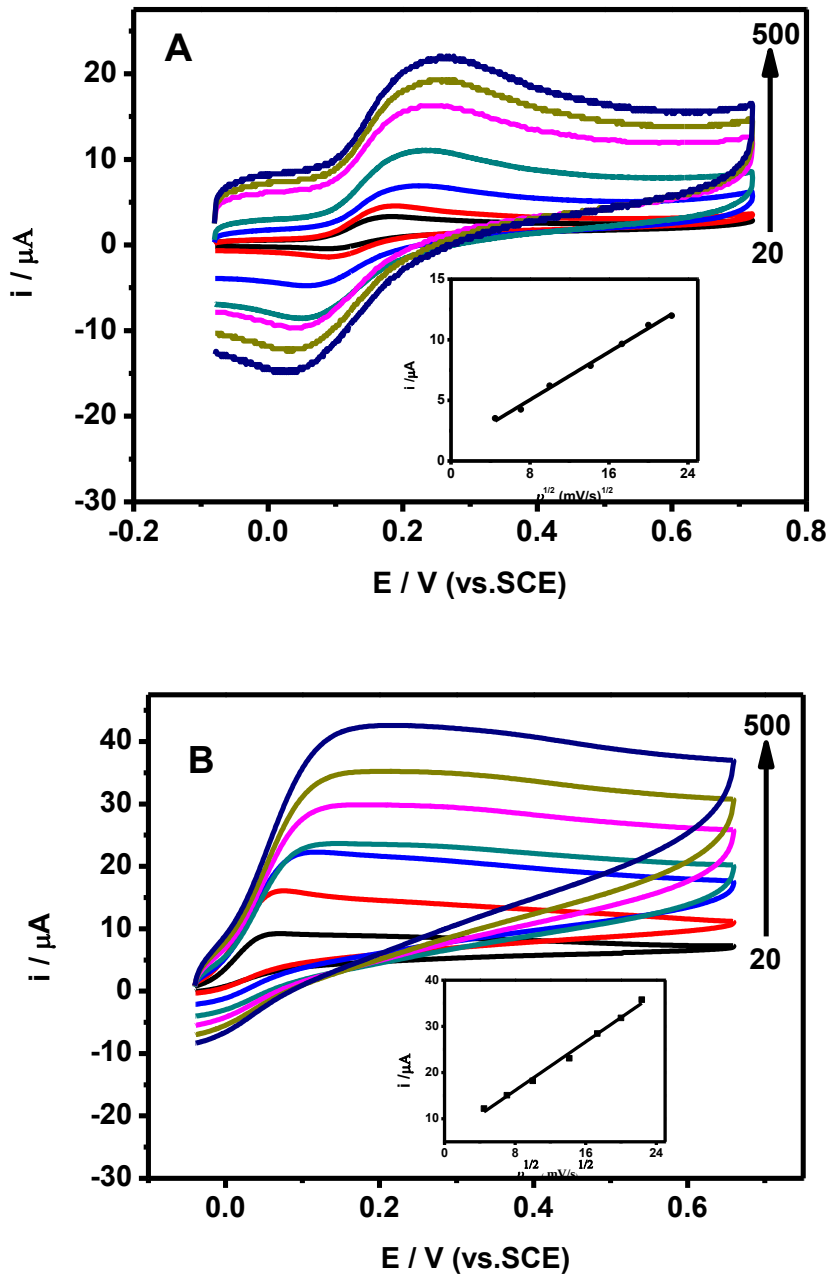

Figure 7. CVs for the oxidation of (A) 0.5 mM DA and (B) 1.0 mM AA at the $(NG/PEI)_5$/GCE in 0.10 M PBS with different scan rate: 20 mV/s, 50 mV/s, 100 mV/s, 200 mV/s, 300 mV/s, 400 mV/s and 500 mV/s.

3.5. Electrochemical determination of DA

Determination of DA is performed by employing the DPV technique at the $(NG/PEI)_5$/GCE for the oxidation of various concentrations of DA in the presence of 500 μM AA in PBS solution. As can be seen in Fig.8, the anodic peak current of DA increases linearly with the increasing concentration of DA from 1.0×10^{-6} M to 1.3×10^{-4} M in the presence of AA, and the detection limit is 5×10^{-7} M (S/N=3). The corresponding linear function is I_{pa}= 0.4804 +0.06144 c_{DA} (R= 0.999).

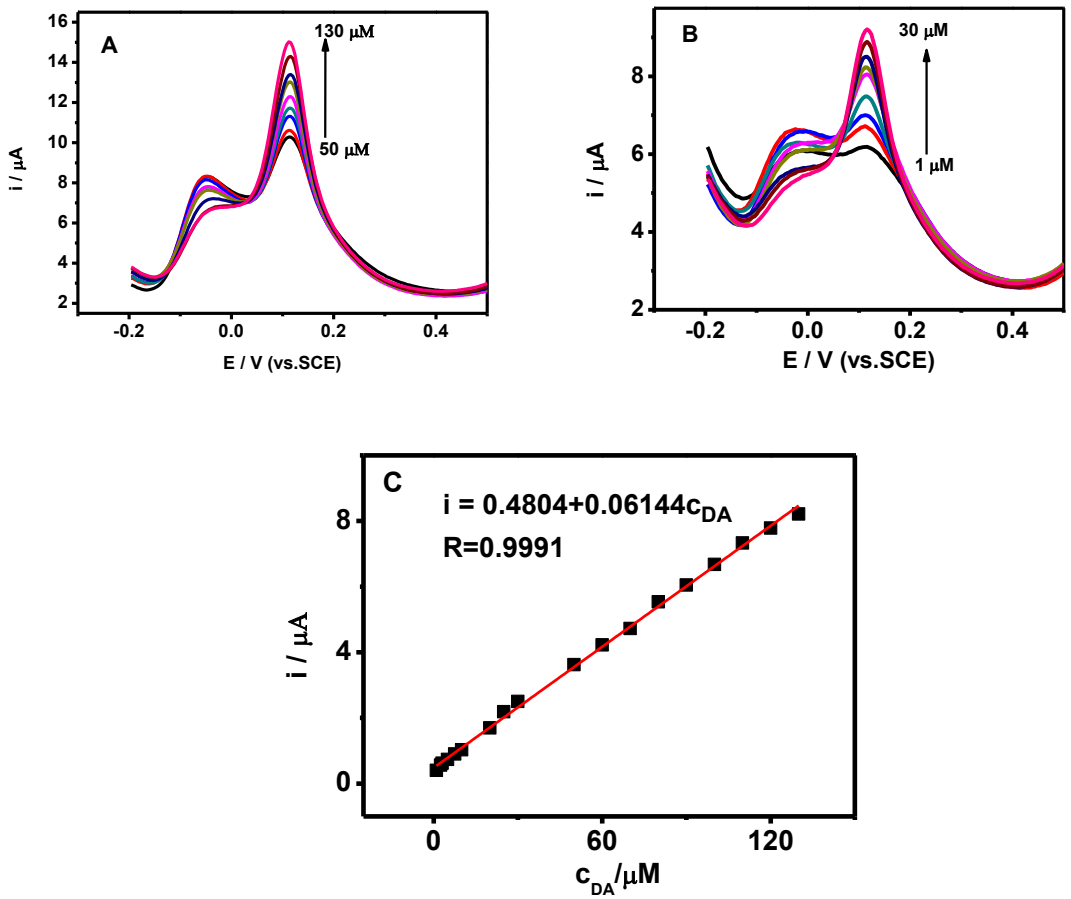

Figure 8. DPV profiles at $(NG/PEI)_5$/GCE in 0.1 M PBS (pH=7.4) containing 500 μM AA and different concertrations of DA from (A) 50 μM to 130μM, (B) 1 μM to 30μM and (C) Plot of the anodic peak current as a function of DA concentration from 1 μM to 130μM.

3.6. Reproducibility and stability

In addition, the stability of the modified electrode has been investigated. The relative standard deviation is 5.4% for five continuous determinations of 1 mM DA. No apparent decrease in the current response was found over 5 days, and about 79% remained after one week and kept almost constant afterward.

4.CONCLUSION

In this work, nitrogen-doped graphene has been prepared and LBL films of these modified nanomaterials have been built up in combination with a polyelectrolyte, PEI, to obtain dense and stable nanocoatings on solid surfaces. It is shown that the modified electrode displayed good reproducibility and favorable sensing performance for the detection of dopamine. The experimental results prove that the LBL assembly method is a viable way to prepare NG sensors.

ACKNOWLEDGEMENTS
Nana Li and Enhui Zheng contributed to this work equally. The authors greatly appreciate the supports of the National Natural Science Foundation of Zhejiang Province (No.LQ12B05002).

References

1. R. M. Wightman, L. J. May and A. C. Michael, *Anal. Chem*., 60 (1988) 769.
2. Bossi, S. A. Piletsky, E. V. Piletska, P. G. Righetti and A. P. F. Turner, *Anal. Chem*. 72 (2000) 4296.
3. X. H. Lin, Y. F. Zhang, W. Chen and P. Wu, *Sens. Actuators B*, 122 (2007) 309.
4. J. F. van Staden and R. I. van Staden. *Talanta*, 102 (2012) 34.
5. U. Yogeswaran, S. Thiagarajan and S. M. Chen, *Anal. Biochem*., 365 (2007) 122.
6. A.A. Ensafi, M. Taei and T. Khayamian, *J. Electroanal. Chem*., 633 (2009) 212.
7. K. Saha, S. S. Agasti, C. Kim, X. Li and V. M. Rotello, *Chem. Rev*., 112 (2012) 2739.
8. M.C. Daniel and D. Astruc, *Chem. Rev*., 104 (2004) 293.
9. M. Stratakis and H. Garcia, *Chem. Rev*., 112 (2012) 4469.
10. L. Sánchez, R. Otero, J. M. Gallego, R. Miranda and N. Martín, *Chem. Rev*., 109 (2009) 2081.
11. G. A. Rivas, M. D. Rubianes, M. C. Rodriguez, N. E. Ferreyra, G. L. Luque, M. L. Pedano, S. A. Miscoria and C. Parrado, *Talanta*, 74 (2007) 291.
12. L. B. Hu, D. S. Hecht and G. Grüner, *Chem. Rev*., 110 (2010) 5790.
13. Y. T. Shieh, Y. C. Tsai and Y. K. Twu, *Int. J. Electrochem. Sci*., 8 (2013) 831.
14. M. S. Artiles, C. S. Rout and T. S. Fisher, *Adv. Drug Delivery Rev*., 63 (2011) 1352.
15. T. Kuila, S. Bose, P. Khanra, A. K. Mishra, N. H. Kim and J. H. Lee, *Biosens. Bioelectron*., 26 (2011) 4637.
16. X. Zhu, Q. Liu, X. H. Zhu, C. L. Li, M. T. Xu and Y. Liang, *Int. J. Electrochem. Sci*., 7 (2012) 5172.
17. M. Y. Chao, X.Y. Ma and X. Li, *Int. J. Electrochem. Sci*., 7 (2012) 2201.
18. G. Aragay, F. Pino and A. Merkoci, *Chem. Rev*., 112 (2012) 5317.
19. K. Yang and B. S. Xing, *Chem. Rev*., 110 (2010) 5989.
20. H. B. Wang, T. Maiyalagan and X. Wang, ACS Catal., 2 (2012) 781.
21. R. Lv and M. Terrones, *Mater. Lett*.,78 (2012) 209.
22. L.S. Panchakarla, A. Govindaraj and C.N.R. Rao, *Inorg. Chim. Acta*, 363 (2010) 4163.
23. Z. H. Sheng, X. Q. Zheng, J. Y. Xu, W. J. Bao, F. B. Wang and X. H. Xia, *Biosens. Bioelectron*., 34 (2012) 125.
24. Y. Wang, Y. Shao, D. W. Matson, J. Li and Y. Lin, *ACS Nano*,4 (2010) 1790.
25. Xiong, Y. K. Zhou, Y. Y. Zhao, J. Wang, X. Chen, R. O'Hayrec and Z. P. Shao,*Carbon*, 52 (2013) 181.
26. J. Hong, J. Y. Han, H. Yoon, P. Joo, T Lee, E. Seo, K. Char and B. S. Kim, *Nanoscale*, 3 (2011) 4515.

27. C. Marcano, D. V. Kosynkin, J. M. Berlin, A. Sinitskii, Z. Z. Sun, A. Slesarev, L. B. Alemany, W. Lu and J. M. Tour, *ACS Nano*, 4 (2010) 4806.
28. X. B. Fan, W. C. Peng, Y. Li, X. Y. Li, S. L. Wang, G. L. Zhang and F. B. Zhang, *Adv. Mater*., 20 (2008) 4490.
29. A.C. Ferrari and J. Robertson, *Phys. Rev. B*, 61(2000) 14095.
30. M. A. Pimenta, G. Dresselhaus, M. S. Dresselhaus, L. G. Cancado, A. Jorio and R. Saito, *Phys. Chem. Chem. Phys*., 9 (2007) 1276.
31. X. B. Fan, W. C. Peng, Y. Li, X. Y. Li, S. L. Wang, G. L. Zhang and F. B. Zhang, *Adv. Mater*., 20 (2008) 4490.
32. L. Sun, L. Wang, C. G. Tian, T. X. Tan, Y. Xie, K. Y. Shi, M. T. Li and H. Fu, *RSC Adv*., 2 (2012) 4498.
33. S. A. Hasan, K. E. Tsekoura, V. Sternhagen, and M. Strømmeand. *J. Phys. Chem. C*, 116 (2012) 6530.
34. C. R. Raj, K. Tokuda and T. Ohsaka, *Bioelectrochemistry*, 53, (2001) 183.